RAPID COMMUNICATIONS

PHYSICAL REVIEW B **94**, 041112(R) (2016)

Offset-corrected Δ-Kohn-Sham scheme for semiempirical prediction of absolute x-ray photoelectron energies in molecules and solids

Michael Walter,[1,2,*] Michael Moseler,[1,2,3] and Lars Pastewka[2,4]

[1] *Freiburger Materialforschungszentrum, Universität Freiburg, Stefan-Meier-Straße 21, D-79104 Freiburg, Germany*
[2] *Fraunhofer IWM, MikroTribologie Centrum µTC, Wöhlerstrasse 11, D-79108 Freiburg, Germany*
[3] *Physikalisches Institut, Universität Freiburg, Herrmann-Herder-Straße 3, D-79104 Freiburg, Germany*
[4] *Karlsruher Institut für Technologie, Institut für Angewandte Materialien, Engelbert-Arnold-Straße 4, D-76131 Karlsruhe, Germany*

(Received 20 November 2015; revised manuscript received 11 May 2016; published 25 July 2016)

Absolute binding energies of core electrons in molecules and bulk materials can be efficiently calculated by spin paired density-function theory employing a Δ-Kohn-Sham (ΔKS) scheme corrected by offsets that are highly transferable. These offsets depend on core level and atomic species and can be determined by comparing ΔKS energies to experimental molecular x-ray photoelectron spectra. We demonstrate the correct prediction of absolute and relative binding energies on a wide range of molecules, metals, and insulators.

DOI: 10.1103/PhysRevB.94.041112

Introduction. X-ray photoelectron spectroscopy (XPS) has become a valuable tool for the characterization of molecules and materials [1,2]. High energy photons ionize the system under study by removing an electron from a core level (see Fig. 1). The resulting energy loss can be interpreted as a direct measure of the core electron binding energy (CEBE). Core levels typically range between several tens [~80 eV for Al(2s)] to hundreds [~570 eV for F(1s)] of eV and this large spread allows for a determination of the elemental composition of materials.

Furthermore, the exact CEBE of an atomic species can vary by several eV, depending on its local chemical environment. This "chemical shift" is an indirect measure for the configuration of the valence electrons that determine the atoms' bonds. It forms the basis of the electron spectroscopy for chemical analysis method [1,2] that is routinely used for chemical material characterization. In practice the assignment of experimental XPS lines relies on extensive tables of CEBEs measured in well-known compounds [3–7]. An *ab initio* prediction of core levels has turned out to be useful for the interpretation of experimental spectra to finer details [8,9]. Such predictions are particularly fruitful for more complicated molecules or solids where atoms of the same elements are present in heterogeneous environments, for instance in minerals and glasses, where local coordination number as well as local bond lengths can vary from one atomic site to the other [10].

In this Rapid Communication, we provide an extensive benchmark of inexpensive density-functional theory (DFT) calculations [11] within the Δ-Kohn-Sham (ΔKS) formalism [12]. We carry out ΔKS calculations of *absolute* CEBEs for isolated systems and explore the potential of periodic ΔKS to reproduce *absolute* CEBEs from solid state XPS experiments. In view of future applications to large material systems we aim at the most efficient scheme and therefore our ΔKS approach is based on spin-paired calculations. We demonstrate below, that in contrast to general belief [13], periodic DFT can be used for the prediction of *absolute* CEBE values with good accuracy. Errors that are associated with the spin-paired treatment and with inaccuracies in the exchange-correlation potential can easily be compensated by offsets $\delta[X(nl)]$ that depend merely on the element type X and the core level nl (e.g., $\delta[C(1s)]$ is the offset of the carbon 1s core level). These highly transferable offsets are virtually independent of the chemical environment of the respective species X and do not vanish for spin-polarized calculations.

Theory. Despite the common interpretation as a single particle energy, the CEBE

$$-E_B = E_0 - E^+_{\mathrm{ch}} \tag{1}$$

is the difference between the ground state energy of a system E_0 and the energy of a (metastable) excited state E^+_{ch} of the same system with one electron less [14,15]. The definition of the ionized core-hole state itself relies on an effective single particle picture and is thus not unambiguous. Nevertheless, the ΔKS method, which defines a core hole as a partly filled Kohn-Sham orbital, has been shown to correlate well with experiment [12,16,17].

A molecular CEBE can be directly compared to experiment as the energy scales of both the neutral ground state and the ionized state that contains the core hole are well defined. The reference energy of such finite systems is the vacuum level $\varepsilon_{\mathrm{vac}} \equiv 0$, i.e., the energy of an electron at infinite distance from the molecule (see Fig. 1). The vacuum level also serves as a convenient reference for the energy needed to remove the most weakly bound valence electron [the ionization potential (V_i)] and for the energy gained by an extra electron [the electron affinity (A_e)]. These many particle energies unambiguously define the single particle energies of the highest occupied (HOMO) and the lowest unoccupied molecular orbital (LUMO), $\varepsilon_H = -V_i$ and $\varepsilon_L = -A_e$, respectively [18]. Equation (1) can be directly applied when the electron is ejected into the vacuum surrounding the molecule.

The vacuum level is not an easily accessible reference for extended systems. There the CEBE is usually reported relative to the Fermi level ε_F [19], which is the energy threshold up to which the single particle levels are filled:

$$E^F_B = E^+_{\mathrm{ch}} - E_0 + \varepsilon_F. \tag{2}$$

---

[*] michael.walter@fmf.uni-freiburg.de

©2016 American Physical Society

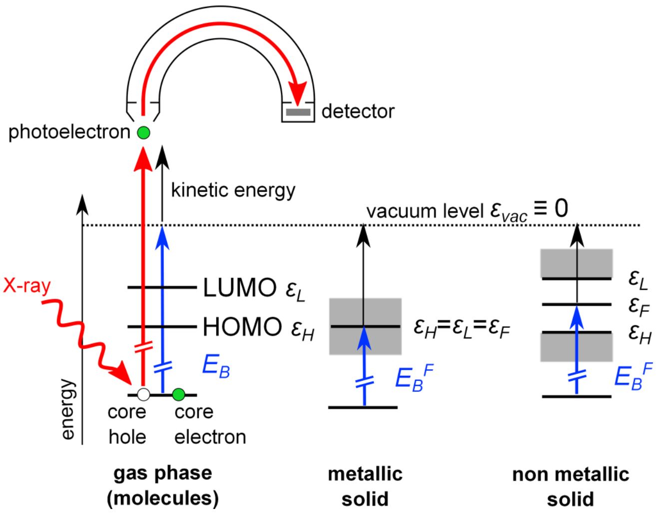

FIG. 1. Schematic presentation of x-ray photoelectron spectroscopy and the relevant energy levels in core hole ionization. The core electron binding energy CEBE $= -E_B$ for molecules and CEBE $= -E_B^F$ for solids.

The charged state energy $E_{\rm ch}^+$ in Eq. (2) poses a problem in simulations as extended systems typically have to be modeled using periodic boundary conditions. These require a neutral unit cell to avoid interaction of the charge with its periodic images. This problem can be overcome by artificially neutralizing the system, by either adding an extra valence electron [13,20,21] or by adding a constant background charge [13,22–24].

Adding a valence electron changes the total energy of the system by the LUMO energy ε_L [25] such that the neutral system containing the core hole has the energy $E_{\rm ch}^0 = E_{\rm ch}^+ + \varepsilon_L$ and the binding energy of the core hole for extended systems becomes

$$E_B^F = E_{\rm ch}^0 - E_0 + \varepsilon_F - \varepsilon_L. \tag{3}$$

In metallic systems, many of the single particle energies coincide as $\varepsilon_F = \varepsilon_H = \varepsilon_L < 0$ (see Fig. 1). In this case, the core hole binding energy relative to the Fermi level simply becomes $E_B^F = E_{\rm ch}^0 - E_0$. This quantity is also straightforward to measure in experiments according to Eq. (2), since for metallic systems the Fermi level is given by the electrostatic potential (voltage) of the metallic specimen.

The situation is more complicated for nonmetals. For systems with a finite band gap $\varepsilon_L - \varepsilon_H$, ε_F lies somewhere inside of the gap. The exact position depends on temperature, is strongly influenced by impurities [26], and can be modified by the presence of surface layers [27]. Measured binding energies for nonmetals therefore tend to vary by many eV from experiment to experiment. Computationally, the situation is further complicated because the empty (Kohn-Sham) energy levels obtained from density-functional theory calculations (based on the usual gradient corrections) are typically too low in energy leading to a significant underestimation of the band gap.

Chemical shifts are independent of these complications since the energy reference cancels out. In application of a chosen single particle picture, these shifts were analyzed by contributions that are attributed to differences between two atomic sites already present in the "initial state" or emergent in the final state of the ionization process [14]. In Kohn-Sham DFT, the method of choice for large molecules and solids due to its computational efficiency, approximate CEBEs are obtained directly from the eigenvalues of core states [28–30]. This approach is especially popular in solid state applications since it circumvents the treatment of charged ionized states in periodic supercells. It was shown, however, that the neglect of relaxation in the final state results in appreciable errors including predictions of erroneous shift directions [20] and prohibits the determination of reliable absolute CEBEs [13]. Within the single particle picture, relaxation effects can be included via Slater-Janak transition state theory, where the orbital energy of a partly occupied core-hole state is interpreted as the CEBE [29,31,32].

In order to fully capture final state effects, Eq. (1) has to be applied. The simplest approach to obtain $E_{\rm ch}^+$ or $E_{\rm ch}^0$ is the $Z+1$ or equivalent-core approximation [33,34], where the excited nucleus is replaced by the next element in the periodic table. This approach is covered by ground state DFT, but assumes the density change to be located exactly at the position of the nucleus. While stretching the DFT's validity [14], the most accurate results are obtained by modeling the core hole as a partly occupied atomic state either in all electron [12,16,21,22,35], effective core, or pseudopotentials, [13,17,20] or within the projector augmented wave method and the frozen core approximation [23,28]. These approaches lead to very similar results and yield differences of around 50 meV [28].

Methods. The following DFT calculations were carried out with the GPAW [37,38] package, an implementation of the projector augmented wave (PAW) method [39]. We use the configuration space grid implementation and apply a grid spacing of 0.2 Å to represent the smooth wave functions unless noted otherwise. The exchange correlation energy was approximated by the generalized gradient correction by Perdew *et al.* (PBE) [40] and additional calculations were carried out in the local density approximation (LDA) [41]. All calculations are spin-paired with the exception indicated. For isolated systems, the size of the simulation box had at least 4 Å vacuum around each atom. Molecules were relaxed until the maximum force dropped below 0.05 eV Å^{-1}.

The wave functions of core atomic states are approximately independent of the chemical environment and can be treated in the frozen core approximation. We freeze the $1s$ electrons for C, N, O, and F, and additionally the $2s,2p$ electrons for Al, Si, P, and S. The atomic Kohn-Sham states are obtained within a non-spin-polarized spherical symmetric approximation. A similar approach is adopted to describe the core hole by lowering the occupation of the relevant state in the atomic calculation by unity. The resulting Kohn-Sham orbitals are then used to construct the frozen core [23,38].

Molecules. We have calculated the $1s$ core-hole binding energies of the elements C, N, O, and F; the $2p$ core-hole energies of Al, Si, P, and S; and the $3d$ core-hole energy of Sn for a total of 78 molecules and 148 chemically distinct core-hole binding energies. Figure 2 shows that there is an excellent linear correlation between calculated and experimental data [42] [see the similar correlation for Sn in

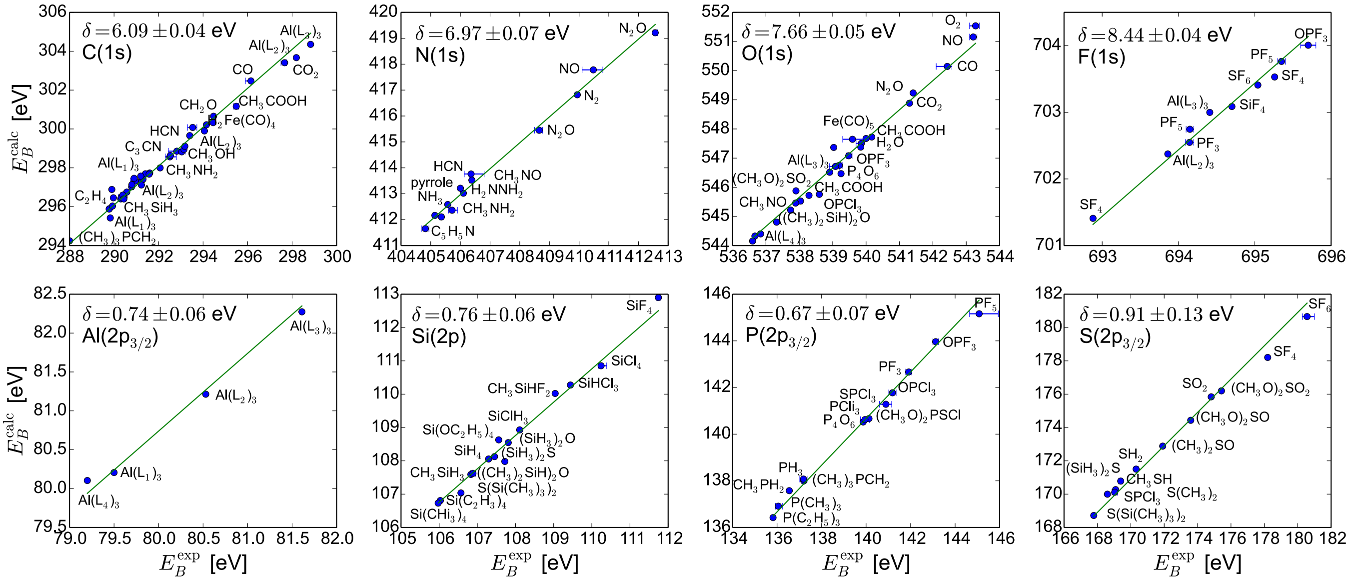

FIG. 2. Core electron binding energies obtained with the PBE functional compared to experimental values for molecules in the gas phase. The constant offset δ for each element corresponding to the straight line is given (see text). The exact numbers are listed in the Supplemental Material [36].

the Supplemental Material (SM) [36]]. The main difference between experiment, E_B^{expt}, and simulation, E_B^{calc}, is a constant offset $\delta = E_B^{\text{calc}} - E_B^{\text{expt}}$ that depends on element and core electron level as demonstrated by the straight lines in Fig. 2. Binding energies typically span several eV over which the deviation from a linear correlation analysis is small.

The values of the offsets δ are given in Fig. 2 and in Table I. The PBE offsets are mostly positive (i.e., E_B is predicted too large), are largest for the $1s$ core holes and increase from C ($\sim$6 eV) to F ($\sim$8.5 eV) as binding energy increases and the core hole becomes more localized. The offset is much smaller ($\sim$1 eV) for the less localized $2p$ core holes in Al, Si, P, and S and becomes negative for the $3d$ core hole of Sn. The standard deviations reported in Fig. 2 are always $\leqslant$0.1 eV. Including the spin dependent core-hole density [23] yields smaller offsets of $\lesssim$1 eV (see Table I). This computationally more demanding approach leads to rather small corrections for the $2p$ holes, but it overcorrects for the more localized $1s$ and $3d$ holes. Table I also shows that δ is strongly dependent on the functional. LDA gives lower values than PBE, while the qualitative trend of increasing values from C to F and lower offsets for $2p$ and $3d$ holes prevails.

Numerical settings influence the values of the offsets [43], where the grid spacing h is found to have the largest influence as can be seen in Table I. The remaining differences to the experiment might have several reasons including dynamic screening effects [24,44], spin-orbit contributions, and inaccuracies of the density functional applied.

The important observation is that the offset δ does depend on just atom type and orbital and is—to a good approximation—independent of molecule and chemical environment. This enables a correction of energies obtained from facile spin-unpolarized calculations for an accurate prediction of absolute core-hole binding energies. The standard deviation of the approach is smaller than 0.2 eV for all elements considered, an accuracy that is sufficient in comparison to the variation over several eV due to differences in the chemical environment. The inclusion of spin does not help to improve the accuracy as can be seen for the example of O_2. Although the spin-paired energy is 1 eV higher than the energy of the paramagnetic solution, the corrected O($1s$) values are similar (543.88 and 543.86 eV). The reason for this similarity can be traced back to the cancellation of spin effects in the energy difference in Eq. (1).

Bulk solids. The δ values parametrized from molecular spectra can now be used to predict CEBEs of bulk solids. We used experimental lattice constants and atomic positions for all solids studied. The complete reference list of the extensive experimental data used in this study is found in the SM [36]. An extra electron was added to the valence band while

TABLE I. Empirical offsets δ in eV between experimental and calculated core-hole binding energies as depicted in Fig. 2.

xc	C	N	O	F	Al	Si	P	S	Sn
PBE	6.07	6.95	7.66	8.44	0.74	0.76	0.67	0.91	−0.27
PBE [a]	6.10	7.12	7.88	8.55	0.74	0.76	0.66	0.87	−0.31
LDA	3.05	3.38	3.60	3.84	0.68	0.72	0.66	0.91	−0.05
PBE [b]	−0.93	−1.12	−1.45	−1.69	−0.02	−0.10	−0.28	−0.13	−1.02

[a] PBE calculation with grid spacing $h = 0.15$ Å.

[b] PBE calculation with corrected spin density (see text).

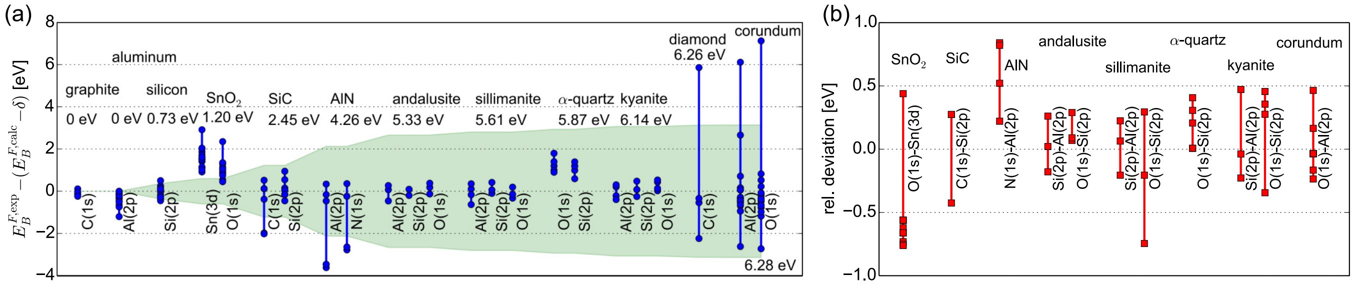

FIG. 3. (a) Difference between experimental $E_B^{F,\mathrm{expt}}$ and calculated $E_B^{F,\mathrm{calc}} - \delta$ for various solids. The numbers quoted and the shaded area give the PBE band gaps of the respective material. (b) Differences of relative shifts between pairs of elements for a certain compound. Multiple points indicate individual experimental results.

keeping the core hole empty and E_B^F was evaluated according to Eq. (3). Figure 3(a) shows the resulting differences between experimental and calculated CEBEs for various solids. Including the offset, we find our calculated *absolute* CEBE to be in excellent agreement with experiment for the semimetal bulk graphite and the metal aluminum, where the Fermi level serves as good reference.

This is not the case anymore for nonmetals as is most obvious for materials with the largest gaps, such as diamond and corrundum, where experimental values spread over many eV. Despite this problem, we find an astonishing agreement even in absolute CEBEs for many systems by setting $\varepsilon_F = (\varepsilon_H + \varepsilon_L)/2$ using PBE values for ε_H and ε_L. This approach is satisfactory compared to the experimental spread for crystalline silicon and diamond as well as crystalline compounds of Al, Si, C, and O, in particular nitrides (AlN), oxides (corrundum), carbides (SiC), and aluminosilicates (andalusite, kyanite, and sillimanite which are polymorphs of Al_2SiO_5). Exceptions are SnO_2 and α-quartz, where the calculated values are too small by roughly 1 eV as compared to experiment.

Energy reference problems cancel out when CEBE differences within a single compound are considered. In this case the experimental energy spread is drastically reduced when values from the same experiment are compared [Fig. 3(b)]. Also the agreement between prediction and experiment is excellent for all solids considered. This shows that the prediction of relative shifts is possible even for systems with large gaps. Note that the empirical energy offsets δ do not cancel since they vary between different elements and core levels and need to be considered even for the calculation of relative shifts.

Summary and discussion. We have presented a convenient computational method for the prediction of absolute CEBEs from DFT calculations within the PAW formulation. A large set of experimental molecular data have been used to show that spin-paired gas-phase calculations predict CEBEs in excellent accuracy up to a constant offset that mainly depends on chemical element and core level. These offsets allow an *a posteriori* correction of DFT results and therefore a prediction of core electron binding energies also for solids. The main issue in absolute CEBEs is the definition of the reference energy, a problem also present in experiment. This mainly affects systems with a band gap, where the common Fermi energy reference is not defined. Chemical shifts that do not require the definition of an energy reference can still be calculated with good accuracy. Moreover, knowing the δ values enables the prediction of relative shifts between different elements within the same material independent of the definition of the Fermi level.

It would be desirable to have δ values for all elements of the chosen functional. Such a database could serve for the assignment of experimental XPS peaks via direct comparison to simulations. Gas-phase XPS spectra can be used for parametrization as shown above. For elements where these are not available, an alternative route is the calibration from metallic alloys where accurate relative shifts are available. Finally, also more accurate, but computationally more demanding quantum chemical calculations could be used to obtain δ without reference to experiment.

Acknowledgments. Computational resources of FZ-Jülich and from the bwHPC-C5 project are gratefully acknowledged. This work is partially based on research funded by the DFG (Grants No. PA 2023/2 and No. MO 879/17).

[1] K. Siegbahn, C. Nording, J. Hedman, P. F. Heden, K. Hamrin, U. Gelius, T. Bergmark, L. Werme, R. Manne, and Y. Baer, *ESCA Applied to Free Molecules* (North-Holland, Amsterdam, 1969).

[2] K. Siegbahn, *Atomic Physics 3* (Springer US, Boston, MA, 1973).

[3] G. Beamson and D. Briggs, *High Resolution XPS of Organic Polymers: The Scienta ESCA300 Database* (Wiley, New York, 1992).

[4] B. Henke, E. Gullikson, and J. Davis, At. Data Nucl. Data Tables **54**, 181 (1993).

[5] J. F. Moulder, W. F. Stickle, P. E. Sobol, and K. D. Bomben, *Handbook of X-ray Photoelectron Spectroscopy* (Physical Electronics, Inc., Eden Prairie, MN, 1995).

[6] B. V. Crest, *Handbook of Monochromatic XPS Spectra* (Wiley, New York, 2000).

[7] A. V. Naumkin, A. Kraut-Vass, S. W. Gaarenstroom, and C. J. Powell, National Institute of Standards and Technology X-ray Photoelectron Spectroscopy Database, 2012, version 4.1, http://srdata.nist.gov/xps/.

[8] P. S. Bagus, Phys. Rev. **139**, A619 (1965).

[9] I. Lindgren, J. Electron Spectrosc. Relat. Phenom. **137-140**, 59 (2004).

[10] H. W. Nesbitt and G. M. Bancroft, Rev. Mineral. Geochem. **78**, 271 (2014).

[11] R. M. Martin, *Electronic Structure* (Cambridge University Press, Cambridge, UK, 2004).

[12] L. Triguero, L. G. M. Pettersson, and H. Ågren, Phys. Rev. B **58**, 8097 (1998).

[13] R. Haerle, E. Riedo, A. Pasquarello, and A. Baldereschi, Phys. Rev. B **65**, 045101 (2001).

[14] W. F. Egelhoff, Surf. Sci. Rep. **6**, 253 (1987).

[15] M. Walter and H. Häkkinen, New J. Phys. **10**, 043018 (2008).

[16] Y. Takahata and D. P. Chong, J. Electron. Spectrosc. Relat. Phenom. **133**, 69 (2003).

[17] O. Takahashi and L. G. M. Pettersson, J. Chem. Phys. **121**, 10339 (2004).

[18] E. J. Baerends, O. V. Gritsenko, and R. van Meer, Phys. Chem. Chem. Phys. **15**, 16408 (2013).

[19] J. Riga, J.-J. Preaux, and J. J. Verbist, Mol. Phys. **34**, 131 (1977).

[20] E. Pehlke and M. Scheffler, Phys. Rev. Lett. **71**, 2338 (1993).

[21] A. Snis and S. F. Matar, Phys. Rev. B **60**, 10855 (1999).

[22] J. Titantah and D. Lamoen, Carbon **43**, 1311 (2005).

[23] M. P. Ljungberg, J. J. Mortensen, and L. G. M. Pettersson, J. Electron. Spectrosc. Relat. Phenom. **184**, 427 (2011).

[24] T. Susi, M. Kaukonen, P. Havu, M. P. Ljungberg, P. Ayala, and E. I. Kauppinen, Beilstein J. Nanotechnol. **5**, 121 (2014).

[25] We regard the LUMO energy ε_L as constant under the addition of the extra electron, an approximation that becomes exact in the limit of infinite supercells.

[26] S. M. Sze, *Physics of Semiconductor Devices*, 2nd ed. (Wiley, New York, 1981).

[27] S. Zhong, J. Q. Zhong, H. Y. Mao, J. L. Zhang, J. D. Lin, and W. Chen, Phys. Chem. Chem. Phys. **14**, 14127 (2012).

[28] L. Köhler and G. Kresse, Phys. Rev. B **70**, 165405 (2004).

[29] A. Gandubert, E. Krebs, C. Legens, D. Costa, D. Guillaume, and P. Raybaud, Catal. Today **130**, 149 (2008).

[30] M. Vogel, C. Kasigkeit, K. Hirsch, A. Langenberg, J. Rittmann, V. Zamudio-Bayer, A. Kulesza, R. Mitrić, T. Möller, B. v. Issendorff, and J. T. Lau, Phys. Rev. B **85**, 195454 (2012).

[31] D. P. Chong, Chem. Phys. Lett. **232**, 486 (1995).

[32] D. P. Chong, J. Chem. Phys. **103**, 1842 (1995).

[33] N. Mårtensson and B. Johansson, Solid State Commun. **32**, 791 (1979).

[34] B. Johansson and N. Mårtensson, Phys. Rev. B **21**, 4427 (1980).

[35] T. Susi, D. J. Mowbray, M. P. Ljungberg, and P. Ayala, Phys. Rev. B **91**, 081401 (2015).

[36] See Supplemental Material at http://link.aps.org/supplemental/10.1103/PhysRevB.94.041112 for tables of molecular XPS spectra and experimental solid state references.

[37] J. J. Mortensen, L. B. Hansen, and K. W. Jacobsen, Phys. Rev. B **71**, 035109 (2005).

[38] J. Enkovaara *et al.*, J. Phys.: Condens. Matter **22**, 253202 (2010).

[39] P. E. Blöchl, Phys. Rev. B **50**, 17953 (1994).

[40] J. P. Perdew, K. Burke, and M. Ernzerhof, Phys. Rev. Lett. **77**, 3865 (1996).

[41] J. P. Perdew and Y. Wang, Phys. Rev. B **45**, 13244 (1992).

[42] W. L. Jolly, K. D. Bomben, and C. J. Eyermann, At. Data Nucl. Data Tables **31**, 433 (1984).

[43] M. Walter, M. Moseler, and L. Pastewka (unpublished).

[44] K. Kotsis and V. Staemmler, Phys. Chem. Chem. Phys. **8**, 1490 (2006).